

Influence of carbon content and processing treatment of metallic binder on the outgassing and sintering of NbC based cemented carbide

Amir Hadian^{a,b,*}, Cyrus Zamani^a, Claudia Schreiner^c, Renato Figi^c, Frank Jörg Clemens^b

^a School of Metallurgy and Materials Engineering, College of Engineering, University of Tehran, Tehran, Iran

^b Empa, Swiss Federal Laboratories for Materials Science & Technology, Laboratory for High Performance Ceramics, 8600, Dübendorf, Switzerland

^c Empa, Swiss Federal Laboratories for Materials Science & Technology, Laboratory for Advanced Analytical Technologies, 8600, Dübendorf, Switzerland

ARTICLE INFO

Keywords:

Thermal analysis
NbC
High speed steel
Cemented carbide
Cutting tools
Composites

ABSTRACT

In this study, two grades of high speed steel (HSS), having different carbon content and processing treatment (i.e. cryo-milling and atomization), were used as a metallic binder for NbC cemented carbides. Thermoanalytical methods were used to investigate the outgassing and sintering of the two NbC cemented carbides during heat treatment. For this mean, thermogravimetry (TG), differential scanning calorimetry (DSC) and evolved gas (EG) analysis during thermal heat treatment were carried out. The results indicated that the processing treatment has a great impact on the thermal behavior of the steel powders, which later can be traced in the thermal behavior of the compacts. Higher decarburization was traced during the thermal analysis on the powder prepared via cryo-milling compared to the one made by the atomization process. From the TG analysis of the green compacts, it was evident that intensive outgassing occurs at temperatures above 850 °C. This phenomenon is associated with the activation of several mechanism in NbC and steel above this temperature which was realized from the evaluation of the initial powders. To gain a deeper understanding on the basic reactions and the effect of carbon content on phase transformations during the thermal process, thermodynamic studies was performed using commercial software (Thermo-Calc). It was evident that decreasing the carbon content shifts the transformation temperatures (e.g. liquid formation) to higher levels. This is especially important in adjusting the sintering temperature in NbC-high speed steel system as sufficient portion of liquid phase should be presented during the sintering process in order to obtain a satisfactory sintering.

1. Introduction

Cemented carbides are widely used tool materials with a general composition of a dominant carbide phase (WC, TiC, NbC, etc.) and a metallic phase (Co, Ni, Fe, etc.) as a binder. The mechanical properties, especially hardness and fracture toughness of these materials are highly dependent on their processing treatment including powder synthesis and processing, green shaping and consolidation process. These steps have widely been explored by researchers while less attention has been directed toward the analysis of the thermal processing step. Early works on thermal analysis of well-known WC-Co hardmetals started by Leitner et al. [1]. They showed that the thermal analysis is a valuable route to understand how to maintain the carbon balance and improve the properties of hardmetals. Deeper analysis by Leitner et al. [2] showed that three processes as dewaxing, outgassing and sintering are identified

during the thermal treatment of hard metal green compacts. The dewaxing process, described as decomposition of hydrocarbon chains, typically occurs at temperatures around 200–350 °C. This is not a delicate step in cemented carbides produced via powder metallurgy as generally less than 3 wt% of an organic binder (e.g. paraffin wax) is introduced inside the green samples and the probability of crack formation is very low. However, according to Upadhyaya [3], rapid dewaxing process and low oxygen content in the furnace atmosphere could result in soot formation and change in the carbon concentration. Based on Upadhyaya [4] studies on materials science of cemented carbides, disrupting the carbon balance within a WC-Co mixtures results in the formation of new phases (graphite or η -phases) which influences both the sintering behavior and the mechanical properties of the final product. The outgassing process, starting from 350 °C, has the most striking effect on the carbon balance. In this step, oxide impurities on the surface

* Corresponding author. Empa, Swiss Federal Laboratories for Materials Science & Technology, Laboratory for High Performance Ceramics, 8600, Dübendorf, Switzerland.

E-mail addresses: a.hadian@ut.ac.ir, amir.hadian@empa.ch (A. Hadian), c.zamani@ut.ac.ir (C. Zamani), frank.clemens@empa.ch (F.J. Clemens).

<https://doi.org/10.1016/j.ceramint.2020.07.347>

Received 5 April 2020; Received in revised form 30 July 2020; Accepted 31 July 2020

Available online 6 August 2020

0272-8842/© 2021 The Authors. Published by Elsevier Ltd. This is an open access article under the CC BY license (<http://creativecommons.org/licenses/by/4.0/>).

of the carbide and metal powder are reduced by the carbon from the mixture (e.g. decomposed binder). Gestrich et al. [5] describes that the reduction processes are greatly influenced by the size of the initial powders as well as the processing treatment on them. The authors show that using ultrafine grained carbide powders and long milling exercises can increase the amount of surface oxides thus amplifying the outgassing process. While the surface oxides are being reduced, highly activated surfaces are produced which triggers the sintering process. To investigate the outgassing phenomenon in cemented carbonitrides, Chen et al. [6,7] suggested the use of a quadrupole mass spectrometer system at the exhaust of the furnace. Under Chen conditions, a three stage CO evolution during the heating process could be observed for WC based on the stepwise reduction of WO_3 surface oxides.

Unlike the WC-Co system, less attention has been directed to the thermal behavior of other groups of cemented carbides. According to Mohrbacher et al. [8] comprehensive evaluation of NbC based cemented carbides for wear applications, these materials are considered as a potential substitute for WC-Co. Recently a growing interest has been directed to incorporate various metallic binders such as Co and Ni in NbC based cemented carbides. Initial works by Woydt and Mohrbacher [9] on tribological properties of cobalt bonded NbC, indicates the enhanced wear resistance of spark plasma sintered NbC–8Co cemented carbide compared to other ceramics and hardmetals, especially at high sliding velocities. Huang et al. [10] discovered that full densification can also be achieved in NbC based cemented carbides using liquid phase sintering. The authors also found that using iron-based metallic binders rather than cobalt results in higher hardness at comparable fracture toughness in pressure-less sintered NbC cemented carbides. Recent attempts by Hadian et al. [11] in using high speed steels (HSS) as a binder indicates the bright prospective in the further development of NbC–Fe cemented carbides. Similar to WC-Co, in NbC–Fe system maintaining the carbon balance is necessary to achieve preferred mechanical properties. This is more crucial in NbC-HSS system as the carbon concentration has a great impact on both the NbC and HSS properties. According to Vinitskii [12], the NbC microhardness is strongly affected by the carbon/metal (C/Me) ratio. When C/Me is around 0.8, a maximum hardness of 2700 kg/mm^2 can be obtained in NbC. Deviation from this ratio (i.e. higher or lower carbon content) results in a dramatic reduction in the hardness. In the case of HSS, the carbon content influences the solidification process, microstructure and mechanical properties. Study on solidification of HSS by Boccalini and Goldenstein [13] shows that carbon has a significant influence on the liquidus and eutectic reactions temperatures. Meanwhile, the solidification sequence can also be affected by the amount of carbon as it stabilizes the austenite phase. Barkalow et al. [14] found that carbon drop can lead to the replacement of austenite by ferrite to be the primary phase to precipitate from the liquid in M2 HSS. Fredriksson and Brising [15] discovered that the effect of carbon content on the microstructure is mainly connected to the morphology and the total volume of the eutectic carbides in the HSS binder. As the mechanical properties rely on microstructural features, these variations in the microstructure can modify the mechanical properties. Previous studies by Wei et al. [16] show that higher carbon content increases the total volume of eutectic carbides which results in higher hardness and reduced toughness.

Based on the knowledge discussed above, understanding the parameters which can affect the carbon balance is necessary to optimize the sintering of these materials and to obtain desired mechanical properties. The aim of this paper is to use thermoanalytical techniques such as differential scanning calorimetry (DSC), thermogravimetry (TG) and evolved gas (EG) analysis using combined gas chromatography and mass spectroscopy (GC-MS) on green NbC-HSS pressed parts to study the effect of processing treatment on thermal behavior. Accordingly, two grades of HSS powder (M48 and M2), having different carbon content and prepared via different processing routes, atomization and cryo-milling, were selected as initial metallic binders. The importance of the milling process in obtaining HSS powders is the simplicity of the

process and being economically more favored against the atomization process when small batches of powder are needed. This is especially important in developing NbC-HSS cemented carbides as limited grades are available in the atomized shape in the market. To obtain a comprehensive understanding of the basic reactions during heating, first the thermal behavior of individual components was analyzed then compacts of NbC-M2 HSS and NbC-M48 HSS were prepared for thermoanalytical studies. Finally, the effect of carbon concentration on the solidification sequence of HSS powders was thermodynamically investigated.

2. Materials and methods

2.1. Sample preparation

NbC powder (d50: $1.02 \mu\text{m}$, Langfeng Metallic, China) and N_2 -atomized M2 HSS powder (90% – $16 \mu\text{m}$ – Sandvik Osprey, UK) were used as the initial components. A cryogenic milling apparatus described by Esmaeilzadeh et al. [17] was used to prepare M48 HSS powders according to the developed procedure by Hadian et al. [11]. M48 HSS was only commercially available in M48 solid rods. Therefore mechanical grinding was used to achieve M48 HSS coarse chips, that were cryogenically milled to obtain fine steel particles. To avoid direct contact of liquid nitrogen with metal powders and possible contamination, a cryo-milling chamber was used with two walls, an inner shell containing the powder and the milling balls and the outer shell which contained liquid nitrogen. The milling process was performed in ethanol for 6 h at -90°C . The as-milled powder was first sieved then dried for 24 h at 50°C before mixing with NbC. To prepare NbC-HSS mixtures, the NbC powder was first subjected to wet-milling to break down the agglomerates. Milling was carried out in a polyethylene bottle for 24 h with a 15:1 ball to powder weight ratio (BPR) in toluene. After milling, 12 wt % of HSS powder and 3 wt% of wax (paraffin wax, Sigma-Aldrich) was added inside the same bottle and mixing was performed at a lower BPR of 5:1 for 12 h. To separate the solvent from the powder mixture, a rotary evaporator (R-134, Buchi, Switzerland) was used at 40°C and 77 mbar. Finally, the powder mixture was formed into pellets with a diameter of 5 mm using a manual hydraulic press (PW 20, P/O/Weber, Germany) at 400 MPa. All dry pressed samples weighted $300 \pm 5 \text{ mg}$.

The green samples were partially debinded before thermoanalytical measurements. For this mean, the samples were held for 1 h at 280°C in a Carbolite tube furnace (STF 16/450) in a flowing argon atmosphere. Using this debinding process, 1.9% of sample weight loss was measured.

2.2. Characterization and thermal analysis

Microstructural observations were carried out on the initial NbC and M2 HSS powders and the cryo-milled M48 HSS using a scanning electron microscope (VEGA3, TESCAN Co., Czech Republic). The particle size distribution of these powders was measured using a laser diffraction particle size analyzer (LS13 320, Beckman Coulter, USA). To measure the chemical composition of the metallic powders, an inductively coupled plasma optical emission spectrometer (Foundry-Master Pro, Oxford Instruments, UK) was used.

For thermal analysis, a DSC-TG instrument (Jupiter F3 STA 449, NETZSCH, Germany) coupled with an gas chromatograph (GC 7890 B, Agilent, USA) - mass spectrometer (MS 5977 B, Agilent, USA) was used to investigate the thermal mass loss and the exhaust gas species. To study the thermal analysis of the initial powders, equal masses (e.g. 85 mg) were used. Constant heating rate of 10 k/min up to 1420°C under a flowing (60 ml/min) argon atmosphere was used for the experiments. For the dry pressed pellets, the exhaust gases were continuously monitored for the specific gas species indicated in Table 1 using the mass spectrometer.

Thermodynamic analysis was facilitated using Thermo-Calc software equipped with TCFE 9 database.

Table 1
Specific mass numbers and associated gas species.

Specific mass number	Main peak	Secondary peak
16	CH ₄	CO, CO ₂ and H ₂ O
17	–	CH ₄
18	H ₂ O	–
28	CO	CO ₂
32	O ₂	–
44	CO ₂	–

2.3. Measurement of carbon and oxygen content

The carbon and oxygen content of the NbC, M2 HSS and M48 HSS powders were measured using an infrared method after fusion/combustion in a furnace. To study the effect of mixing process on the concentration of C and O, similar measurements were performed on the NbC-M48 HSS and NbC-M2 HSS mixtures as well.

For the quantitative determination of carbon, 1 g of sample was melted in an induction furnace (CS 844, LECO, USA) at 2000 °C in an oxygen stream using a mixture of 2 g tungsten and tin (LECOCEL-II) as melting aids. The element of interest, carbon, was detected in an infrared measuring cell as CO₂. The determinations were carried out according to ISO 15350 standard for the steel powders.

For the determination of oxygen, 0.5 g of sample was melted in a graphite crucible in an electrode furnace (ONH 836, LECO, USA) using 0.4 g of nickel chips as melting aid at 3000 °C. Oxygen was released and could be quantified as CO₂ using an infrared measuring cell. The

determinations were carried out following the ISO 17053 standard for the steel powders. For each powder/mixture, the C and O measurements were performed on 2–4 samples to obtain a standard deviation.

3. Results and discussion

3.1. Characteristics of the starting materials

The morphology of the as-received NbC, the M2 HSS, and the cryogenic milled M48 HSS powders are shown in Fig. 1. In Fig. 2, the particle size distribution of these powders are presented. As can be seen in Fig. 1 (a), NbC fine powders have an irregular morphology and a great tendency to form agglomerates which indicates the necessity to perform a prolonged initial milling process. From the particle size analysis (Fig. 2 (a)), it is evident that most of the NbC particles are in the sub-micron regime. On the other hand, the micron-sized M2 HSS powders (Fig. 1 (b)) are spherical due to the atomization process and do not form agglomerates. To preserve this shape during the mixing process, a low BPR and short milling time as described in section 3.1 were selected in order to obtain a homogenous mixture of NbC and HSS powders.

From Fig. 1 (c) and (d), the effect of cryo-milling on coarse M48 HSS chips obtained from a mechanical grinding process can be seen. The reduction in the particle size achieved from the cryo-milling process is accompanied by a morphology change to flake-like particles. Comparing the particle size distribution, the M48 HSS powders have a broad distribution compared to M2 HSS atomized powders which is related to the flake-like morphology of the M48 HSS powders. In Table 2, the chemical

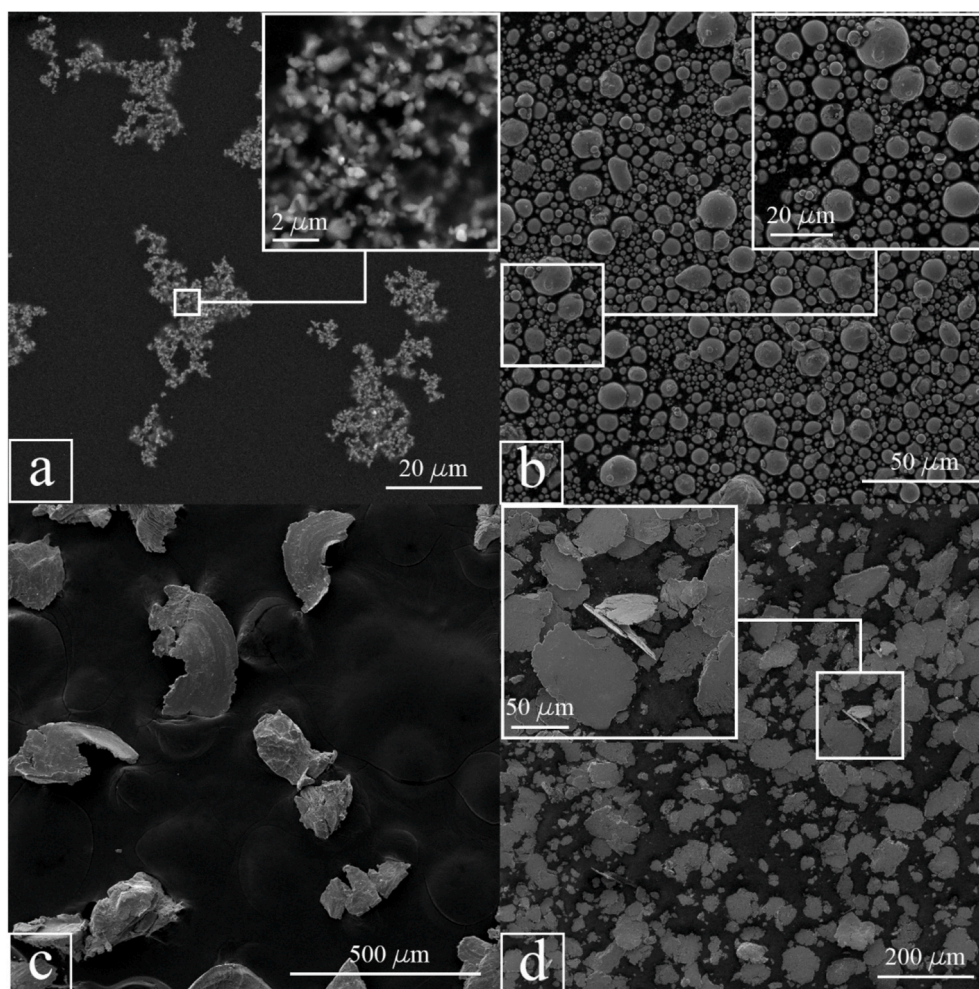


Fig. 1. Scanning electron microscopy of the as-received (a) NbC and (b) M2 HSS powders, M48 HSS powders (c) after mechanical grinding and (d) after cryo-milling.

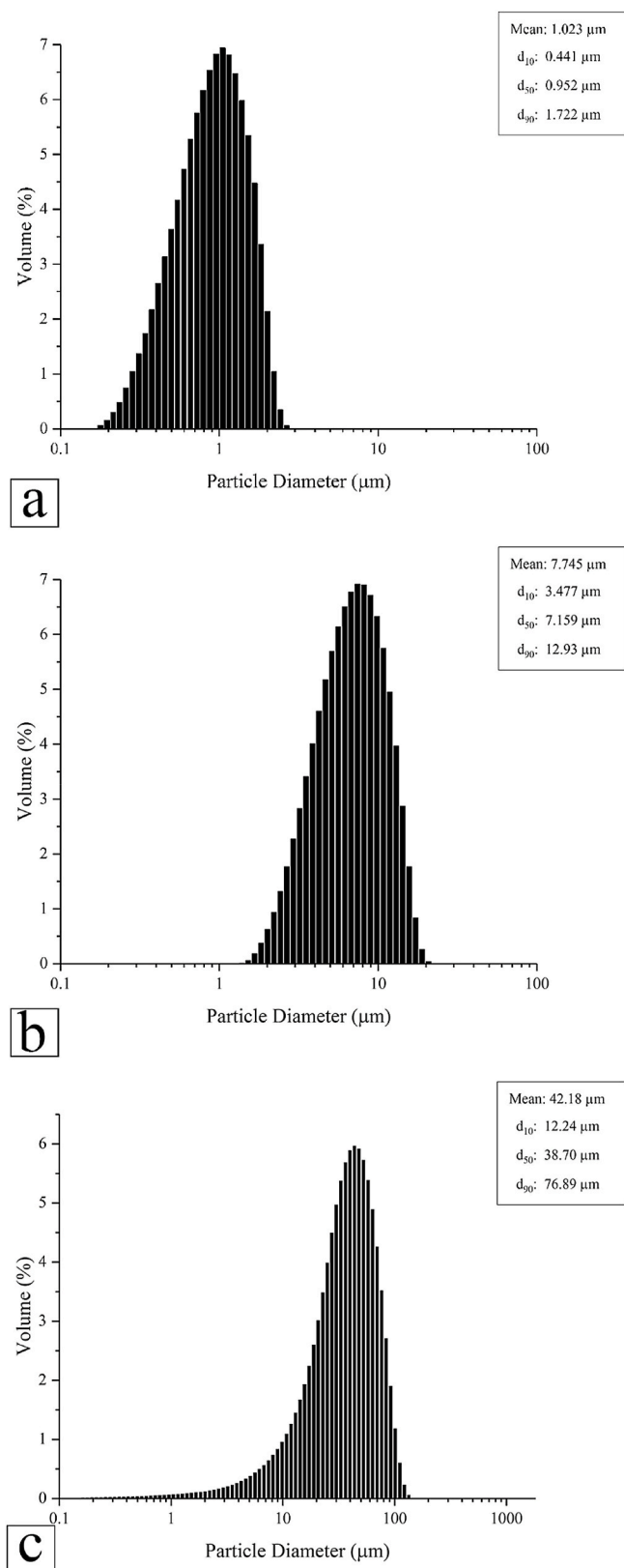


Fig. 2. Particle size distribution of (a) NbC, (b) atomized M2 HSS and (c) cryo-milled M48 HSS powders.

composition of the M2 and M48 powders are presented according to the inductively coupled plasma optical emission spectrometer (ICP-OES) analysis.

3.2. Thermal analysis

To comprehensively understand the thermal analysis of NbC-HSS mixtures, the thermal analysis of the individual components was first evaluated. In the following sections, first the thermal analysis of the three components NbC, M2 HSS and M48 HSS will be discussed and later compared with the thermal analysis of the NbC-HSS pressed mixtures.

3.2.1. Thermal analysis of NbC powder

Fig. 3 presents the DSC (differential scanning calorimetry), TG (thermogravimetry) and DTG (differential thermal gravimetry) measurements as a function of temperature for the NbC powder in flowing argon atmosphere. A constant weight loss can be identified in the TG signal up to 1000 °C followed by a sharp drop at higher temperatures. The initial weight loss is attributed to the reaction of free carbon inside the NbC powder with the oxygen impurities from the protecting atmosphere which results in the formation of CO and CO₂ gases. The presence of free carbon results from the NbC powder synthesis. Typically, the carbon content is usually adjusted slightly higher than the stoichiometric ratio to avoid the formation of NbC_{1-x} compositions. At 1000 °C, the mass starts to decrease faster. In this region, the DSC analysis shows an endothermic peak at 1040 °C (No. 1, Fig. 3) which fits with the carbothermal reduction temperature of Nb₂O₅ Eq. (1).



The results of oxygen content measurements of NbC powder (Table 3), confirms the presence of 0.7 wt% oxygen inside the powder. Considering this analysis and the temperature of detected mass loss in the TG analysis, it is clear that some Nb₂O₅ exists in the starting NbC powder. According to the literature, this reaction will take place at around 970 °C [18]. Based on previous studies by Mohrbacher et al. [8], the carbothermal reaction of NbC is kinetically more favorable in the gas-solid phase state (Eq. (2)) when the so-called Boudouard reaction (Eq. (3)) is involved. The carbothermal reaction in Eq. (2) typically occurs above 1000 °C, which fits nicely with our experiments.



3.2.2. Thermal analysis of the two HSS powders

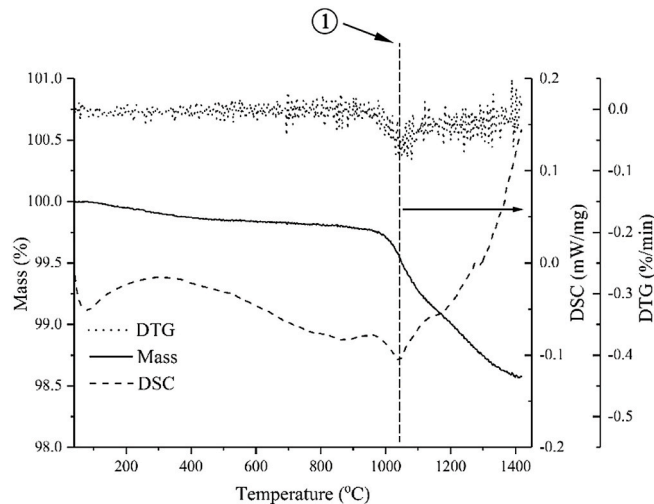
The simultaneous thermal analysis of M48 HSS and M2 HSS powders are shown in Figs. 4 and 5, respectively. Considering the thermal analysis of M48 HSS, a sharp endothermic peak (No. 1, Fig. 4) can be identified in the DSC signal around 850 °C. According to Basu et al. [19] results, this peak indicates the beginning of ferrite to austenite phase transformation. Before this peak, a gentle mass loss is observed and can be explained by the reduction of surface oxides by the carbon inside the steel structure. Looking on the DSC results, a broad endothermic peak can be observed above 850 °C (No. 2, Fig. 4) which is associated with a sharp decrease in mass according to TG signal. Based on previous studies [20], this peak can be explained by the dissociation of M₂₃C₆ and M₆C eutectic carbides and the release of disassociated carbon into the structure. This carbon can move freely inside the austenite phase and migrate to the surface of the particles to react with surface oxides. This process is responsible for the accelerated mass loss in this step. Finally, the formation of liquid phase above 1250° is evident from the endothermic peaks at the end of the DSC results (No. 3, Fig. 4).

The atomized M2 HSS powder behaves very similar to the previously discussed M48 HSS powder. However, some differences can be noted which are associated with the processing treatment and the synthesis of this powder. Unlike the M48 HSS powder, no sign of initial weight loss

Table 2

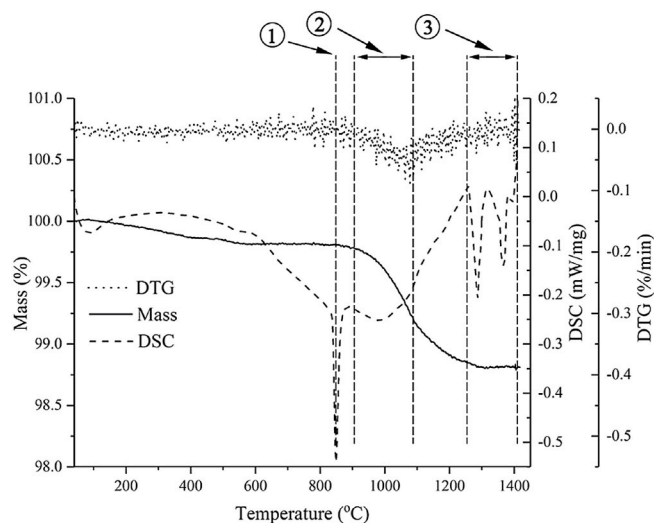
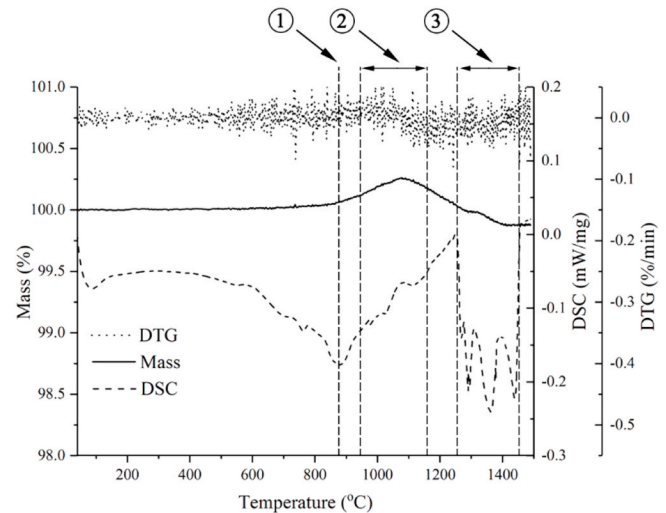
Chemical composition of the steel powders according to the ICP-OES analysis.

Steel type	Element wt%										
	C	Si	Mn	Cr	Mo	Ni	Co	Cu	V	W	Fe
M48 HSS	1.17	0.3	0.3	4.01	3.71	0.2	9.53	0.13	3.02	9.66	Balance
M2 HSS	0.8	0.25	0.21	4.19	5.1	–	–	–	1.97	6.61	Balance

**Fig. 3.** DSC, TG and DTG of NbC powder obtained during heating process up to 1420 °C (10 k/min, flowing argon atmosphere).**Table 3**

Quantitative analysis of C and O content inside HSS and NbC-HSS powders based on an infrared method after fusion/combustion.

Sample	Carbon (wt.%)	Oxygen (wt.%)
NbC powder	11 ± 0.1	0.7 ± 0.05
M48 HSS powder	1.33 ± 0.01	0.5 ± 0.01
M2 HSS powder	0.86 ± 0.01	0.1 ± 0.01
NbC-12 wt% M48 HSS mixture	12.4 ± 0.4	1.8 ± 0.02
NbC-12 wt% M2 HSS mixture	12.1 ± 0.3	1 ± 0.01

**Fig. 4.** DSC, TG and DTG of M48 HSS cryo-milled powder obtained during heating with 10 k/min up to 1420 °C in flowing argon atmosphere.**Fig. 5.** DSC, TG and DTG of M2 HSS atomized powder obtained during heating with 10 k/min up to 1490 °C in flowing argon atmosphere.

can be detected in the M2 HSS powder. The use of the atomization process to synthesis M2 powder and the high cooling rates in this process significantly reduces the chance of oxidation. However, in the case of M48 HSS powder, more metal oxides are presented on the powder surface due to the processing treatment. The results of the quantitative analysis of C and O presented in Table 3 confirms the lower oxygen content of M2 HSS (i.e. 0.1 wt%) compared to M48 HSS (i.e. 0.5 wt%) powder. Based on previous studies by Witkin and Lavernia [21], heavy deformation induced by prolonged cryo-milling process increases the density of dislocations, vacancies and grain boundaries inside the particles. These crystal defects not only facilitate the diffusion of solute elements into the matrix but also decrease the diffusion distance thus enhancing chemical reactions such as oxidation. Meanwhile, the formation of a high density of dislocation ledges on the surface of the particles throughout the cryo-milling process, not only provides higher surface area but also introduces more active sites for oxidation.

A slight mass gain can be detected in the TG signal subsequent to the transformation of ferrite to austenite (No. 1, Fig. 5). It is assumed that some oxidation takes place at this stage due to the presence of oxygen impurities from the flowing protecting atmosphere. According to Bautista et al. [22] findings, ferritic structures are less susceptible to high temperature oxidation compared to austenitic structure. Therefore, the oxidation has occurred after the phase transformation inside the HSS particles from ferrite to austenite. The mass gain is interrupted by a mass loss at higher temperatures (No. 2, Fig. 5) due to the reduction of the as-formed oxides by the free carbon inside the structure.

The influence of the processing treatment can be noted in the DSC measurements as well. Comparing the ferrite to austenite transformation peak (No. 1, Fig. 5) with M48 HSS, here a moderate peak is observed for M2 HSS powder. This phenomenon can also be noted for the endothermic peak related to disassociation of the eutectic carbides (No. 2, Fig. 5) which is weaker in the case of M2 HSS. As stated previously, during the atomization process, the extreme cooling rate restricts the equilibrium phase transformations. Consequently, the incomplete transformation of austenite to ferrite during the cooling process leads to

the presence of retained austenite in the structure. Therefore, the phase transformation of ferrite to austenite occurs with a lower intensity during the heating process. A similar effect can be explained regarding the disassociation of eutectic carbides. Similar to M48 HSS thermal analysis, at the final stage of the DSC signal, signs of liquid formation can be identified from the endothermic peaks (No. 3, Fig. 5).

3.2.3. Thermal analysis of NbC-HSS cemented carbides

In Fig. 6, the data of the simultaneous thermal analysis are presented for NbC-M48 HSS (Fig. 6 (a)) and NbC-M2 HSS (Fig. 6 (b)) pressed pellets. Besides, gas analysis was performed on the exhaust gases evolved from the NbC-M2 HSS sample during thermal analysis experiment. The results are presented in Fig. 7 for selected mass numbers. Each of these mass numbers are characteristic peaks of identical gas species, which are explained in detail in Table 3.

As a general perception, the thermal behavior of NbC-M48 HSS and NbC-M2 HSS are analogues. As the processing treatment of the metallic binders are dissimilar, some differences can be noted in the thermal analysis of the two mixtures which will be discussed in the following section. However, as the steel binders only consist 12 wt% of the total mixture, sharp variations in the DSC and TG signals of the two mixtures are not expected. Five important thermal effects can be characterized in the thermal behavior of NbC-HSS which are highlighted in Fig. 6.

3.2.3.1. Binder removal (below 500 °C). Below 500 °C, a sharp drop in

the TG signal can be seen (No. 1, Fig. 6). It is well known, that this drop is attributed to the decomposition of the organic binder and the residual organic solvents from the mixture. As stated in the experimental part, the samples were partially debinded prior to thermal analysis. However, some residues remain inside the structure which decomposes during the thermal analysis at elevated temperatures. The results from the evolved gas analysis (EGA), confirm this phenomenon as an increase in m18, m28 and m44 species can be observed in this region. Based on the NIST database, these signals can be found in the mass spectrum of paraffin and toluene thus confirm the decomposition process.

3.2.3.2. Outgassing (500 °C–700 °C). In this region (No. 2, Fig. 6), the samples start to lose weight as a second step which corresponds to two endothermic peaks in the DSC signal. As no mass lost was detected in the thermal analysis of NbC and HSS powders at this temperature, it can be concluded that this drop is a result of powders interaction. Looking at the EGA results, the evolution of CO (Fig. 7 (a)) and CO₂ (Fig. 7 (e)) is evident. As stated in section 3.2.2, mechanical milling can assist chemical reactions by the introduction of defects inside the structure of the particles. It is therefore assumed that the mixing process is responsible for the formation of a thin oxide layer on the surface of the mixed powders. This layer can react with the free carbon from the NbC powder during the heating process leading to the evolution of CO and CO₂ gases. The low intensity of DSC peaks confirms that the oxidation is mainly taking place on the surface of the metallic particles which have lower content inside the mixture.

3.2.3.3. Outgassing (above 900 °C). As mentioned in section 3.2.2, the endothermic peak in the DSC analysis (No. 3, Fig. 6) could be explained by the phase transformation from ferrite to austenite. Subsequent to this effect, a broad peak can be noted in the DTG results (No. 4, Fig. 6) in both samples indicating a higher mass loss rate in this region. According to the previously discussed thermal analysis of NbC and HSS powders, several reactions are probable in this region as follow: 1- reduction of Nb₂O₅ by free carbon from the NbC powder 2- release of free carbon inside the HSS powders due to the disassociation of eutectic carbides 3- enhanced mobility of carbon inside the HSS particles due to the presence of austenite phase inside the structure. Along with these effects, the presence of trapped air inside the porosities of the pellets during compaction is a source of oxygen which increases the carbon loss of the samples. Due to these reactions, a comparably high amount of CO evolves from the samples (Fig. 7 (a)). Three CO peaks can be identified in the high CO emission region about 900–1200 °C. A similar outgassing behavior was reported for WC-Co cemented carbides in the literature which was described by the step-wise reduction of tungsten oxides (WO₃, WO_{2.9}, WO_{2.7}, WO₂, W₃O) [7,23]. Likewise, the reduction of niobium oxides (Nb₂O₅, NbO₂, NbO) occurs in different stages [24]. Therefore, it can be assumed that each peak represents the formation of a specific oxide structure.

Considering the final mass of both samples, a comparably high amount of mass loss (i.e. 2 wt % for NbC-M48 HSS & 1.93 wt % for NbC-M2 HSS) is measured after the removal of the organics by the end of the thermal analysis. According to the EGA analysis, the evolution of CO and CO₂ species (Fig. 7 (a)) is mainly responsible for the aforementioned mass loss. Based on the knowledge discussed earlier, controlling the carbon balance inside the structure is vital to achieve desired mechanical properties and to control the sintering process in the NbC-HSS cemented carbides. The later will be discussed in the following section (4.3) in detail. It is therefore essential to either compensate this loss by adding free carbon to the initial mixture or by optimizing the sintering process such as using static protecting atmosphere. It can also be concluded from the values of mass loss in the NbC-M48 HSS and NbC-M2 HSS samples that the processing treatment does not have a major role in adjusting the final carbon content. Slightly higher mass loss observed in NbC-M48 HSS samples is associated with the cryo-milling of the M48

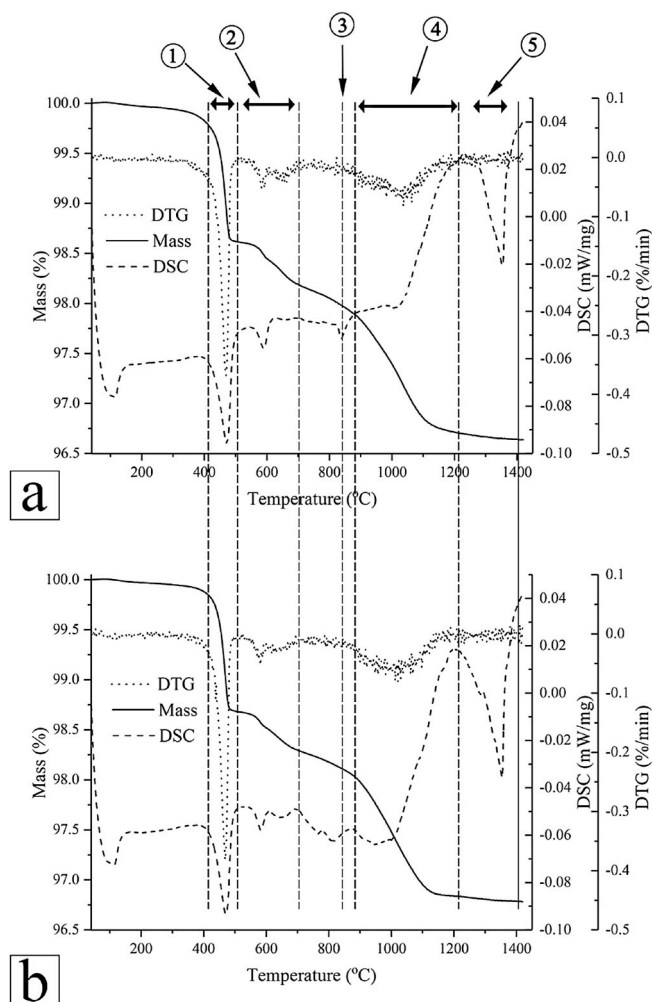


Fig. 6. DSC, TG and DTG of: (a) NbC-12 wt % M48 HSS and (b) NbC-12 wt % M2 HSS green compacts obtained during heating with 10 k/min up to 1420 °C in flowing argon atmosphere.

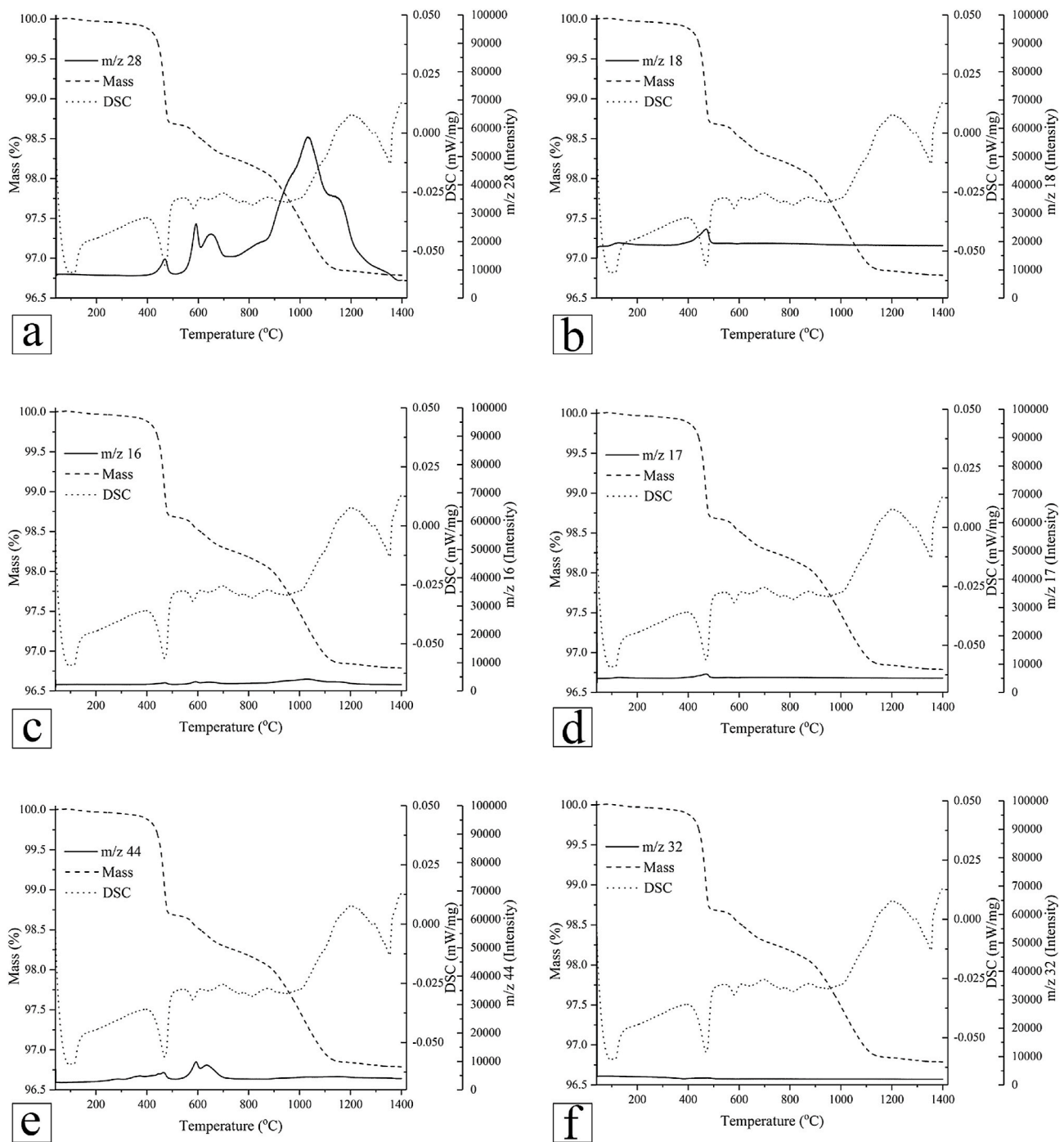


Fig. 7. Variation of: (a) m28, (b) m18, (c) m16, (d) m17, (e) m44 and (f) m32 mass number intensities as a function of temperature synchronized with DSC and TG of NbC-M2 HSS green compact.

HSS powder and the presence of more surface oxides.

3.2.3.4. Liquid formation. In the final stage of the thermal analysis (No. 5, Fig. 6 (b)) a drop in the DSC signal is observed in both cases which indicates the formation of the liquid phase.

3.3. Thermodynamic

As mentioned earlier, in NbC-HSS cemented carbides, the carbon content has significant importance as it influences both the mechanical and microstructural properties of the NbC matrix and the steel binder. Regarding the steel binder, special attention should be directed to

maintain the carbon balance as the temperatures of phase transformations are also affected by the variation of carbon content which can affect the sintering process. In Fig. 8, the effect of decarburization can be noted on the phase evolution of M48 HSS system. From the phase diagram, it is clear that the variation of carbon content on this scale will not influence the phase transformation sequence. However, from phase evolution graphs (Fig. 8 (b) and (c)), it is evident that lower carbon content leads to an increase in transformation temperatures. This supports previous findings by Alvaredo et al. on Ti(C,N)–Fe based cermets [25,26]. Combining the thermoanalytical and thermodynamic studies, they reported a decrease in solidus and liquidus temperatures by increasing the carbon content inside the steel matrix. In other words, at a

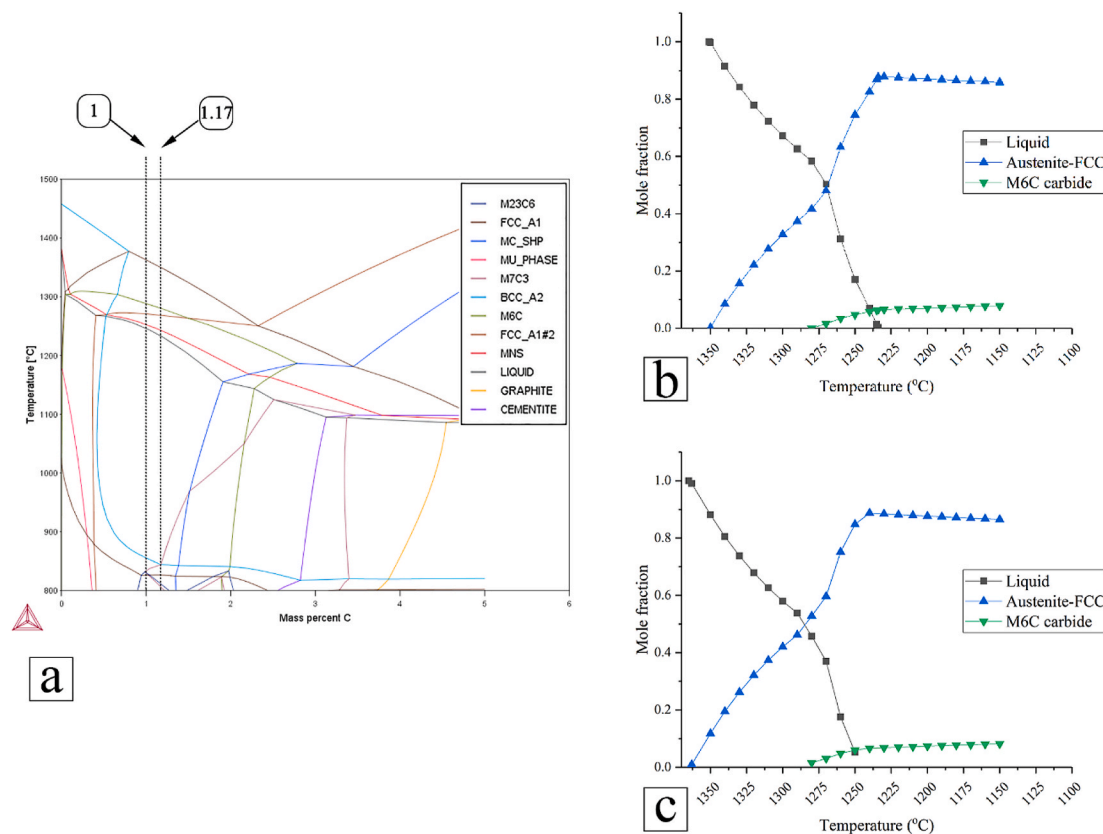


Fig. 8. M48 HSS phase evolution with temperature: (a) calculated phase diagram, (b) and (c) molar fraction of phases versus temperature for M48 HSS containing 1.17 wt % and 1 wt % carbon respectively.

specific temperature, the steel with higher carbon content, contains a higher ratio of liquid phase. Based on Hadian et al. [11] work, lower liquid content which causes a higher viscosity in the liquid phase at the sintering temperature can debilitate the sintering performance. With this in mind, the important role of the carbon content in adjusting the sintering temperature can be acknowledged.

The effect of decarburization on phase evolution of M2 HSS has been calculated and presented in Fig. 9. As a general perception, it can be noted that ferrite is the first solid to precipitate from the liquid phase in M2 HSS while in the case of M48 HSS, austenite precipitates first. Similar to M48 HSS, the variation in carbon content influences the transformation temperatures but no variation in phase transformation sequence can be detected.

In order to have an estimation of the amount of carbon loss during the thermal process, the results of thermodynamic studies are compared with the thermal analysis regarding the liquid formation temperatures in Table 4. As explained in section 3.2.2, during the thermal analysis some decarburization has occurred due to the interaction of carbon with surface oxides, which causes carbon deficiency. This leads to an increase in phase transformation temperatures which is evident in both steels. As higher decarburization was observed in M48 HSS due to the processing treatment, the temperature differences are more notable in this case. Comparing the analytical and experimental results, it can be concluded that the amount of carbon lost during the thermal analysis is less than 0.2 wt%. This can be found out by comparing the liquid formation temperatures measured from the thermal analysis and the thermodynamic data. The explained results define the thermodynamic analysis as a powerful tool to measure the carbon loss inside the steel binder during the heating process.

4. Conclusion

This study focused on thermal analysis of NbC-M48 HSS and NbC-M2 HSS green compacts by thermoanalytical methods in order to optimize the processing of cemented carbides. Based on the analysis of the initial components, it is clear, that the processing treatment greatly influences the decarburization and evolution of CO and CO₂ gases during the thermal treatment. Accordingly, for the M48 HSS powder, the higher oxide content formed during the cryo-milling assists the decarburization process during the heating resulting in a higher mass loss. This effect was less notable for the M2 HSS powder as an atomization process using N₂ protecting gas was used for powder preparation. Therefore, to control the carbon balance, it is necessary to add additional carbon to the powder mixture when long milling practices are performed on the initial powders.

Higher carbon loss was measured for the NbC-HSS pressed pellets compared to separated powders. It is postulated that trapped air inside the porosities of green samples can be a source of oxygen facilitating the decarburization process. It is therefore assumed that vacuuming the sintering chamber for extended period before the heating process would reduce the carbon loss.

By employing thermodynamic calculations (Thermo-Calc software), it was clear that the carbon content inside the metallic binder has a key role in phase transformation temperatures particularly the liquid formation. This is especially important in adjusting the sintering temperature in NbC-HSS cemented carbides as a satisfactory fraction of liquid phase should be presented to ensure the desired sintering process. Comparing the temperature of liquid formation in both systems obtained from theoretical and experimental studies, it was evident that the thermodynamic analysis is a powerful tool to estimate the amount of carbon loss in the metallic binder during the heating process. By comparing the calculated temperatures for phase transformations from

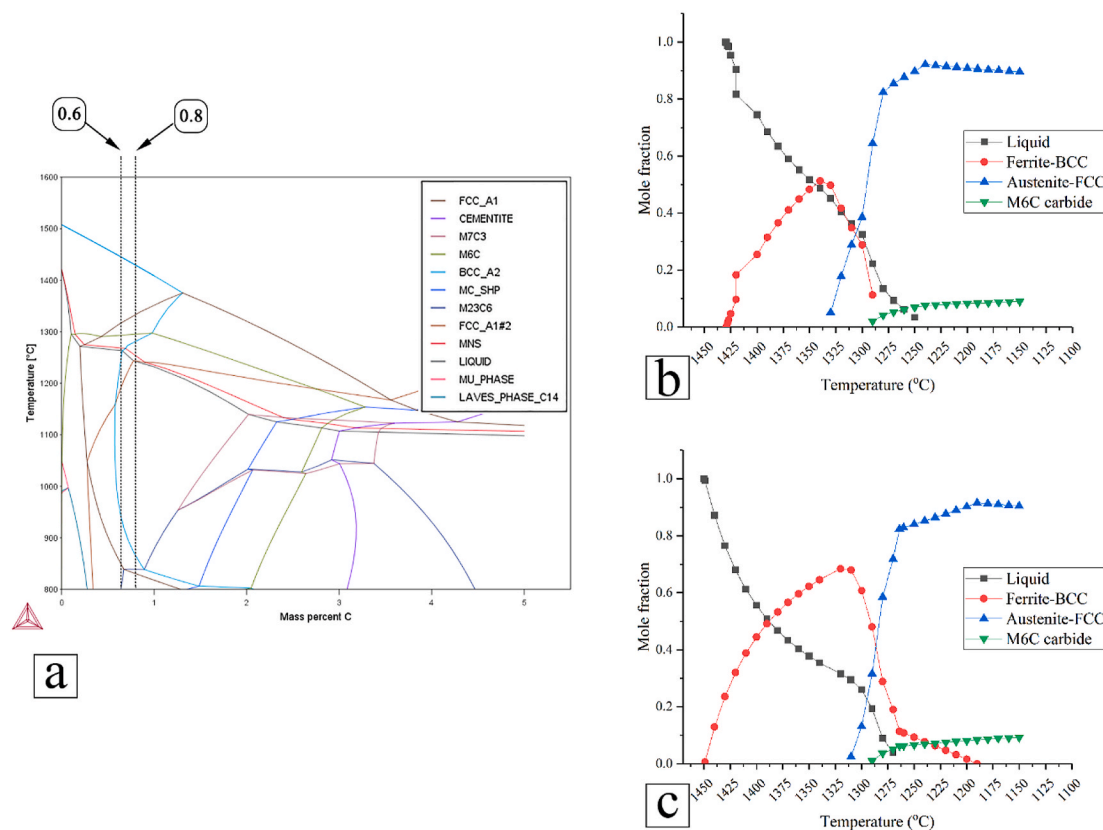


Fig. 9. M2 HSS phase evolution with temperature: (a) calculated phase diagram, (b) and (c) molar fraction of phases versus temperature for M48 HSS containing 0.8 wt % and 0.6 wt % carbon respectively.

Table 4

Comparison of liquid formation temperatures obtained from thermodynamic studies and thermal analysis for M48 HSS and M2 HSS.

Steel	Phase transformation	Thermal analysis (°C)	Thermodynamic (°C)
M48 HSS	Start of liquid formation	1260	1234
	Complete liquid presence	1396	1351
M2 HSS	Start of liquid formation	1275	1250
	Complete liquid presence	1439	1429

thermodynamic studies with those from thermal analysis, it was assumed that less than 0.2 wt% of carbon is lost during the thermal cycle.

Declaration of competing interest

The authors declare that they have no known competing financial interests or personal relationships that could have appeared to influence the work reported in this paper.

Acknowledgments

The authors gratefully acknowledge the financial supports received from the University of Tehran as a scholarship, internal funding from Empa – Swiss Federal Laboratories for Materials Science & Technology and funding for the instrument from SNF project No. 206021 164024.

References

- [1] G. Leitner, K. Jaenicke-Rossler, T. Gestrich, T. Breuning, Thermal analysis aids sintering of hardmetals, *Met. Powder Rep.* 52 (1997) 32–37.
- [2] G. Leitner, T. Gestrich, K. Jaenicke-Rossler, Sintering OF hardmetals-thermoanalytical simulation, *Powder Metall. Prog.* 4 (2004) 179–191.
- [3] G.S. Upadhyaya, *Cemented Tungsten Carbides: Production, Properties and Testing*, William Andrew, 1998.
- [4] G. Upadhyaya, Materials science of cemented carbides — an overview, *Mater. Des.* 22 (2001) 483–489, [https://doi.org/10.1016/S0261-3069\(01\)00007-3](https://doi.org/10.1016/S0261-3069(01)00007-3).
- [5] T. Gestrich, K. Jaenicke-Roessler, G. Leitner, Investigation of processes during sintering of hardmetal by means of thermal analysis, in: *Eur. Congr. Exhib. Powder Metall. Eur. PM Conf. Proc.*, The European Powder Metallurgy Association, 2006, p. 145.
- [6] L. Chen, W. Lengauer, K. Dreyer, Advances in modern nitrogen-containing hardmetals and cermets, *Int. J. Refract. Metals Hard Mater.* 18 (2000) 153–161.
- [7] L. Chen, W. Lengauer, P. Ettmayer, K. Dreyer, H.W. Daub, D. Kassel, Fundamentals of liquid phase sintering for modern cermets and functionally graded cemented carbonitrides (FGCC), *Int. J. Refract. Metals Hard Mater.* 18 (2000) 307–322.
- [8] H. Mohrbacher, M. Woydt, J. Vleugels, S. Huang, Niobium carbide—an innovative and sustainable high-performance material for tooling, friction and wear applications, *Adv. Mater. Sci. Environ. Energy Technol.* V. 260 (2016) 67.
- [9] M. Woydt, H. Mohrbacher, The use of niobium carbide (NbC) as cutting tools and for wear resistant tribosystems, *Int. J. Refract. Metals Hard Mater.* 49 (2015) 212–218, <https://doi.org/10.1016/j.jirmhm.2014.07.002>.
- [10] S.G. Huang, K. Vanmeensel, H. Mohrbacher, M. Woydt, J. Vleugels, Microstructure and mechanical properties of NbC-matrix hardmetals with secondary carbide addition and different metal binders, *Int. J. Refract. Metals Hard Mater.* 48 (2015) 418–426, <https://doi.org/10.1016/j.jirmhm.2014.10.014>.
- [11] A. Hadian, C. Zamani, F.J. Clemens, Effect of sintering temperature on microstructural evolution of M48 high speed tool steel bonded NbC matrix cemented carbides sintered in inert atmosphere, *Int. J. Refract. Metals Hard Mater.* 74 (2018) 20–27, <https://doi.org/10.1016/j.jirmhm.2018.02.021>.
- [12] I.M. Vinitskii, Relation between the properties of monocarbides of groups IV–V transition metals and their carbon content, *Sov. Powder Metall. Met. Ceram.* 11 (1972) 488–493.
- [13] M. Boccalini, H. Goldenstein, Solidification of high speed steels, *Int. Mater. Rev.* 46 (2001) 92–115, <https://doi.org/10.1179/095066001101528411>.
- [14] R.H. Barkalow, R.W. Kraft, J.I. Goldstein, Solidification of M2 high speed steel, *Metall. Trans.* 3 (1972) 919–926.
- [15] H. Fredriksson, S. Brising, Formation of carbides during solidification of high-speed steels, *Scand. J. Metall.* 5 (1976) 268–275.

- [16] S. Wei, Z. Jinhua, X. Liujie, L. Rui, Effects of carbon on microstructures and properties of high vanadium high-speed steel, *Mater. Des.* 27 (2006) 58–63.
- [17] R. Esmailzadeh, M. Salimi, C. Zamani, A.M. Hadian, A. Hadian, Effects of milling time and temperature on phase evolution of AISI 316 stainless steel powder and subsequent sintering, *J. Alloys Compd.* (2018).
- [18] M.W. Chase Jr., NIST-JANAF thermochemical tables, *J. Phys. Chem. Ref. Data, Monogr.* 9 (1998).
- [19] A. Basu, B.K. Ghosh, S. Jana, S.C. Dasgupta, Effect of metallurgical variables on grain size of high-speed tool steels, *Met. Technol.* 7 (1980) 151–158, <https://doi.org/10.1179/030716980803286937>.
- [20] A.F. Rousseau, J.G. Partridge, Y.M. Gözüokara, S. Gulizia, D.G. McCulloch, Carbon evolution during vacuum heat treatment of High Speed Steel, *Vacuum* 124 (2016) 85–88.
- [21] D.B. Witkin, E.J. Lavernia, Synthesis and mechanical behavior of nanostructured materials via cryomilling, *Prog. Mater. Sci.* 51 (2006) 1–60.
- [22] A. Bautista, F. Velasco, M. Campos, M.E. Rabanal, J.M. Torralba, Oxidation behavior at 900° C of austenitic, ferritic, and duplex stainless steels manufactured by powder metallurgy, *Oxid. Metals* 59 (2003) 373–393.
- [23] T. Gestrich, A. Kaiser, J. Pötschke, J. Meinel, S. Höhn, Thermal behaviour of cermets and hardmetals during debinding and sintering, *Int. J. Refract. Metals Hard Mater.* 73 (2018) 210–214.
- [24] N.N. Greenwood, A. Earnshaw, *Chemistry of the Elements*, Elsevier, 2012.
- [25] P. Alvaredo, D. Mari, E. Gordo, High temperature transformations in a steel-TiCN cermet, *Int. J. Refract. Metals Hard Mater.* 41 (2013) 115–120.
- [26] P. Alvaredo, S.A. Tsipas, E. Gordo, Influence of carbon content on the sinterability of an FeCr matrix cermet reinforced with TiCN, *Int. J. Refract. Metals Hard Mater.* 36 (2013) 283–288.